Available online at www.sciencedirect.com
SCIENCE DIRECT®
Journal of Power Sources 142 (2005) 18–26
JOURNAL OF POWER SOURCES
www.elsevier.com/locate/jpowsour

On the use of ammonia electrolysis for hydrogen production

Frédéric Vitse, Matt Cooper, Gerardine G. Botte*

Department of Chemical Engineering, Stocker Center 183, Ohio University, Athens, OH 45701, USA

Received 18 August 2004; accepted 30 September 2004
Available online 30 December 2004

Abstract

An ammonia alkaline electrolytic cell for the production of hydrogen is presented. Challenges involved in using ammonia electro-oxidation for sustainable, low-cost, high-purity hydrogen production are identified and solutions are proposed. Electrodeposition was selected as a technique of preparing low-loading ammonia electrocatalysts. The efficiency of the electrolytic cell was improved by using bimetallic electrodeposited catalysts (at both electrodes) containing Pt and a low concentration of secondary metals (Ru, Ir). Pt–Ir deposits showed the highest activity toward ammonia oxidation. An experimental procedure is shown which minimizes the reversible deactivation of the electrode. Significant current densities were obtained (above 100 mA cm^{-2}) during electrolysis testing at relatively low metal loading, low cell voltages, and high cell efficiencies. These results point to ammonia electrolysis as a promising candidate for an alternative process for low-cost, low-temperature, high-purity hydrogen production.

Keywords: Ammonia electrolysis; Alkaline fuel cell; Hydrogen production; Electrodeposition; Bimetallic catalyst; Water reduction

1. Introduction

1.1. Ammonia as a hydrogen carrier

Hydrogen is the main fuel source for power generation with fuel cells, but its storage and transportation are still major issues. To overcome these problems, hydrogen has been stored and transported via other chemical compounds, such as alcohols, hydrocarbons, ammonia, etc. In many ways, ammonia is an excellent hydrogen carrier [1]; liquid ammonia represents a convenient way of storing supplies of hydrogen, boasting a specific energy density (kW h l^{-1}) 50% higher than liquefied hydrogen [2]. Ammonia is also easily condensed at ambient temperature (under 8 bar of pressure), which makes it a good choice for transportation and storage. Even though ammonia is flammable within defined limits (16–25% by volume in the air) and toxic (above 25 ppm), its presence can be detected by its characteristic odor (above 5 ppm). Ammonia is produced worldwide in large quantities (more than 100 million ton $year^{-1}$), which allows the effect of economy of scale on the cost of production. Its decomposition by electro-oxidation in alkaline media at low overpotentials is NO_x and CO_x free with nitrogen and water as products of reaction [3].

1.2. Electro-oxidation of ammonia: thermodynamics

The original idea presented here consists in coupling the ammonia electro-oxidation reaction with the hydrogen evolution reaction for the production of high-purity hydrogen in an alkaline electrolytic cell [4]:

$$2NH_3(aq) + 6OH^- \rightarrow N_2(g) + 6H_2O + 6e^- \quad (1)$$

$$6H_2O + 6e^- \rightarrow 3H_2(g) + 6OH^- \quad (2)$$

$$2NH_3(aq) \rightarrow N_2(g) + 3H_2(g) \quad (3)$$

At 25 °C the ammonia oxidation potential is −0.77 V versus standard hydrogen electrode (SHE), only 0.06 V less negative than the value of −0.83 V versus SHE for hydrogen evolution in alkaline solution [5]. Therefore, thermodynamic values are much in favor of the production of hydrogen coupled to the oxidation of ammonia compared to hydrogen pro-

* Corresponding author. Tel.: +1 740 593 9670; fax: +1 740 593 0873.
E-mail address: botte@ohio.edu (G.G. Botte).

0378-7753/$ – see front matter © 2004 Elsevier B.V. All rights reserved.
doi:10.1016/j.jpowsour.2004.09.043

duction by electrolysis of water, for which the theoretical cell voltage is 1.223 V. The advantage of this process is its ease of integration with renewable energy (electricity) sources. Because the energy consumption is low, the cell could operate with renewable energy (or by stealing part of the energy of a PEM hydrogen fuel cell if the ammonia electrolytic cell operates close to the theoretical potential). Therefore, hydrogen could be produced on demand, minimizing the needs for hydrogen storage. The theoretical energy consumption during ammonia electrolysis (assuming that there are not kinetics limitations for the reaction to take place at the thermodynamics conditions) can be calculated from the standard potential of the cell and is equal to 1.55 W h g^{-1} H_2 while the electrolysis of water requires at least 33 W h g^{-1} H_2 at standard conditions; this means that theoretically the electrolysis of ammonia consumes 95% lower energy than a water electrolyzer. The scalability of the technology as well as its ability to easily operate in an on-demand mode facilitates the technology's ability to interface with renewable energy sources including those whose production of electricity may vary with time (e.g., wind and solar energy).

1.3. Hydrogen production from ammonia electrolysis: technological challenges

It appears that significant current densities can be obtained from the oxidation of ammonia on platinized Pt (Eq. (1)), but this electrode process is far less reversible (high anodic overpotentials) than the oxidation of hydrogen [6,7]. Apart from the fact that large anodic overpotentials are needed to drive Eq. (1), the deactivation of the Pt-catalyst is quickly observed at higher current densities [8–10]. Therefore, hydrogen production from ammonia electrolysis requires the development of improved catalysts for ammonia electro-oxidation.

In the past, several metals and alloys have been considered as potential catalysts. A study on bulk platinum and bulk iridium electrodes [11] showed that these metals have the best activity among noble and coinage metals toward ammonia oxidation. However, the current densities observed on these catalysts were very low (less than 1 mA cm^{-2}). Metal alloys, metal oxides, and bimetallic electrocatalysts have shown higher activity toward ammonia oxidation compared to monometallic catalysts. This is the case for Ag–Pb alloys [11] and Ru oxides [12] but at very high overpotentials. Co-deposited Pt–Ru electrocatalysts with a low percentage of ruthenium (15 wt.%) have been reported to show higher activity than platinum black at a lower overpotential [13]. A platinum–iridium powder mixture (50 wt.%) impregnated in Teflon and painted on a platinum screen was found to provide much lower overpotentials for the oxidation of ammonia than platinum black [14]. However, the loading of noble metals used (up to 51 mg cm^{-2}) prohibits the use of such technology from an economical point of view.

Studies on amperometric sensors also showed improved sensitivity with respect to ammonia oxidation [15] on electrodeposited noble polymetallic catalysts, but again, low current densities were reported. Recently, Endo et al. [10] optimized the composition of thermally decomposed and melt grown Pt–Ir and Pt–Ru catalysts. The authors concluded that the composition of the deposit cannot alone explain the change in activity observed for the selected catalysts and that the microstructure of the deposit should also be considered and optimized. They also report a fast deactivation of the developed electrocatalysts. Independent results [16] support the fact that the catalysts microstructure plays a significant role on the kinetics of ammonia oxidation and report particularly low overpotential on Pt(1 0 0).

1.4. Objectives of the study

This paper presents some preliminary results showing the technology of hydrogen production from ammonia electrolysis in alkaline solution according to Eq. (3). The objective of this work was to evaluate the feasibility of such a process, which involved the following tasks: (1) the preparation of suitable catalysts for ammonia oxidation by co-electrodeposition of low-loading noble metals, (2) the determination of the purity of hydrogen produced by the process, (3) the improvement of the cell efficiency, and (4) the improvement of the stability of ammonia electro-oxidation reaction. Electrodeposition was selected as a mean of preparing low-loading electrocatalysts, since it is a technique which is relatively easy to implement at an industrial scale.

2. Experimental/materials and methods

2.1. Experimental setup and procedure

A three-electrode 1-L cell was designed for the purpose of electrochemical experimentation. The reference electrode was Hg/HgO (+0.092 V versus SHE), and the counterelectrode was made of platinum–ruthenium foil. The cell includes three additional ports for gas inlet and outlet, and for temperature/pH measurements. The cell could either function as a one-compartment cell or a two-compartment cell. When anodic and cathodic compartments were separated, a polypropylene membrane was used, which provided good conductivity and allowed for the separation of anodic and cathodic gases. Both electrodes were immersed in the solution. All the results shown in this paper were performed in this cell.

An Arbin cycler BT2000 was used for the electrochemical studies. Gas chromatography was performed with an SRI gas chromatograph equipped with a thermal conductivity detector, a HYSEP® column, and a Mole Sieve® column. Additional characterization of the electrodeposit was obtained with scanning electron microscopy (SEM). Rutherford backscattering spectroscopy (RBS) analysis of the samples was performed with a 3.05-MeV 4He beam from the 4.5-MV tandem accelerator in the Edwards Accelerator Labo-

ratory of Ohio University. The beam was scattered through 1680 into a solid-state silicon barrier detector. Beam was incident perpendicular to the sample's surface. The beam energy and scattering angle were chosen to enhance the scattering from oxygen. X-ray photoelectron spectroscopy (XPS) was performed on the samples using Al K X-rays from a dual-anode X-ray source on a Kratos XSAM800 electron spectrometer, part of the W.M. Keck Thin Film Characterization Facility in the Edwards Accelerator Laboratory of Ohio University.

2.2. Solutions, substrate, and electrode preparation

The objective of the electrodeposition procedure was to manage the composition of the bimetallic deposits with small amounts of secondary metals (Ir, Ru). In this way, the influence of the electrodeposited secondary metal on the efficiency of the electrolytic cell can be investigated. Deposits were obtained from the following precursor salts: chloroplatinic acid, ruthenium trichloride, and iridium trichloride. Hydrochloric acid was added as an electrolyte. The substrate used was a 22 mm × 12 mm platinum foil spot-welded to a platinum wire and supported by glass tubing according to the procedure described by Ives and Janz [17]. The substrate was pretreated in aqua regia and cycled in 0.5 M sulfuric acid for removal of impurities as described elsewhere [18]. During the plating procedure, the plating cell was immersed in an ultrasonic bath to improve the integrity of the deposit [19].

The electroplating solution was composed of 1:2.5 Pt–Ru by mass. In another electroplating solution, the Pt–Ir mass ratio was set at 1:1. The selected ratios in the bath solutions provided deposits with around 10% atomic concentration in Ru and Ir. A solution containing only chloroplatinic acid was also used. The deposition current density was set to 5 mA cm^{-2} and the corresponding potential was in a range of −0.3 to −0.1 V versus SHE, far inside the hydrogen evolution region. By doing this, it was expected that a more porous deposit would be obtained. The loading of the electrodes was kept at 2.5 mg cm^{-2}, which is considered a low loading for the electro-oxidation of ammonia when compared to the open literature on catalysts for this reaction (loadings of up to 51 mg cm^{-2} have been reported [14]).

3. Results and discussion

3.1. Characterization of the deposits

The atomic composition for each catalyst is reported in Table 1. Both iridium and ruthenium deposited in smaller amounts than platinum (around 10%). Rough deposits were obtained when platinum was deposited from solutions containing only chloroplatinic acid (Pt electrode) or with low ruthenium content (Pt–Ru electrode). SEM imaging confirmed a rough structure for these two electrodes (Fig. 1a and b, respectively) whereas smoother and denser deposits were obtained with Pt–Ir mixtures (Fig. 1c). This was probably due to the fact that Pt–Ir deposition occurred at comparatively higher potentials and less deep into the hydrogen evolution region. The topography of Pt and Pt–Ru electrodes were very similar; the rough deposits poorly adhered to the substrate. In contrast, the smoother and denser Pt–Ir deposit strongly adhered but had a tendency to flake as the electrode aged.

Table 1
Nomenclature and atomic composition of the electrodeposited catalysts

Electrode name	Mass ratio (plating solution)	Composition of the deposit (atomic percentage)
Pt black	Pt only	100% Pt
Pt–Ru	1/2.5 Pt–Ru	13% Ru, rest Pt
Pt–Ir	1/1 Pt–Ir	10% Ir, rest Pt

The bath composition was adjusted to obtain low concentration of secondary metals (Ru and Ir).

3.2. Gas production and analysis

Nitrogen was produced on Pt, Pt–Ru, and Pt–Ir anodes, while hydrogen was produced on a Pt–Ru cathode. Hydrogen and nitrogen were collected as separate streams when a two-compartment cell was used. In Fig. 2 it is seen that the molar flow rate of produced hydrogen is precisely proportional ($R^2 = 0.998$) to the rate at which electrons are passed between the electrodes of the electrolytic cell. The slope of the linear fit is 0.5, which means that for each hydrogen molecule produced two electrons are passed. This is in agreement with a 100% faradaic efficiency for Eq. (1), for which the same ratio of 0.5 is found (three hydrogen molecules are produced as six electrons are passed).

The equipment used for gas chromatography described in Section 2.1 is capable of detecting trace amounts of CO_x and NO_x (1 ppm). Ammonia present in sufficient quantities (2000 ppm) could also be separated by the HYSEP® column

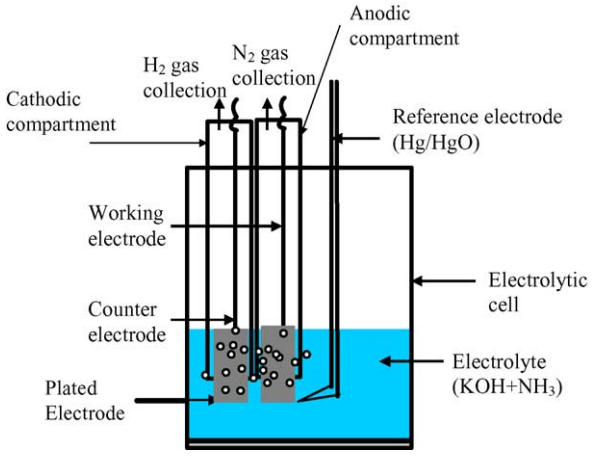

Fig. 1. Scanning electron photomicrographs. Magnification: 1000×, voltage: 30 kV: (a) on Pt black electrode, a rough deposit is observed; (b) on Pt–Ru electrode, rough deposit is observed as well; (c) Pt–Ir with a smoother, denser morphology.

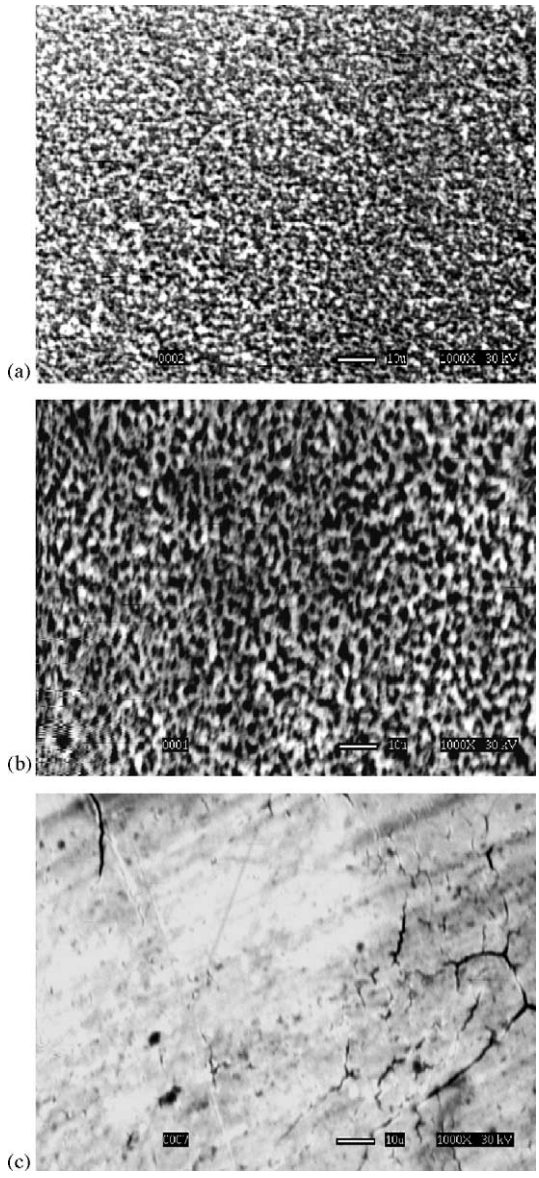

Fig. 2. Hydrogen production rate showing that the reaction represented by Eq. (2) boats a 100% faradaic efficiency (slope is 0.5).

and identified by an ill-defined peak with a retention time slightly shorter than water. When produced hydrogen and nitrogen streams were analyzed, no CO_x, NO_x, or ammonia was detected.

In order to confirm that very low ammonia concentrations carried with the hydrogen gas stream, the cathodic stream was bubbled through HPLC water at 25 °C and the pH of the water was monitored over time. The pH of the HPLC water began to increase as soon as the gas started bubbling and reached a stable value after a few hours (see Fig. 3).

The recorded pH value was 8.4 (after 5 h) when hydrogen was produced in the electrolytic cell at 65 °C. Assuming that water–liquid equilibrium exists between the bubbling water and the gas stream, ammonia concentration in the gas phase could be calculated [20] and was found to be below 1 ppm.

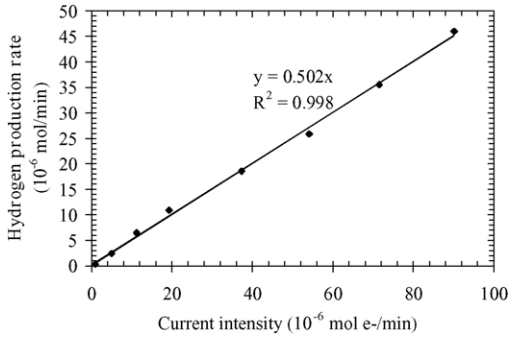

Fig. 3. pH of the bubbling water with respect to time as produced hydrogen is bubbled through. pH is used to calculate the concentration of ammonia in the liquid and gaseous phase under the assumption of vapor–liquid equilibrium.

These low concentrations (<5 ppm) were confirmed by the lack of the characteristic odor of ammonia in the gas stream. These tests prove that ammonia electrolysis at low temperatures has the potential to produce high-purity hydrogen for fuel cell applications. Because both electrodes (anode and cathode) are immersed in the same solution, as shown in Fig. 4, the amounts of ammonia carried with the N_2 stream are similar to the ones carried with the H_2 stream.

3.3. Improvement of the efficiency of the electrolytic cell

3.3.1. Anodic polarization curves

Fig. 5 shows the polarization curves of anodes made of Pt black, Pt–Ru, and Pt–Ir at 60 °C. The current densities reported were measured (arbitrarily) 3 min after a potentiostatic step at the potential of interest started.

At 60 °C, current densities of about 70 mA cm^{-2} are obtained on Pt–Ir at an overpotential of 0.36 V compared to an overpotential of 0.56 V on Pt black. Pt–Ru activity was somewhat intermediate between Pt black and Pt–Ir, showing lower overpotentials than Pt black but a higher overpotential than Pt–Ir. The maximum current density obtained on Pt–Ir at 60 °C was an order of magnitude larger than that observed on Pt black. The better results observed on bimetallic electrodeposited catalysts can be explained in view of the mechanism proposed by Gerischer and Mauerer [8]:

$$NH_{3,ads} + OH^- \Leftrightarrow NH_{2,ads} + H_2O + e^- \quad (4.1)$$

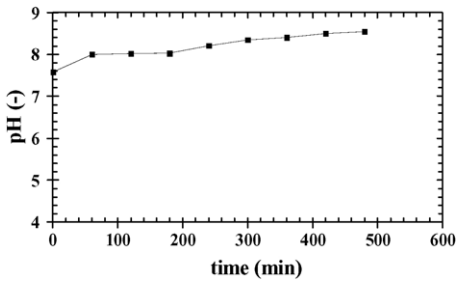

Fig. 4. Three-compartment electrolytic cell for the electrolysis of ammonia. All the experiments reported in the paper were performed in this cell. The electrodes are immersed in the solution.

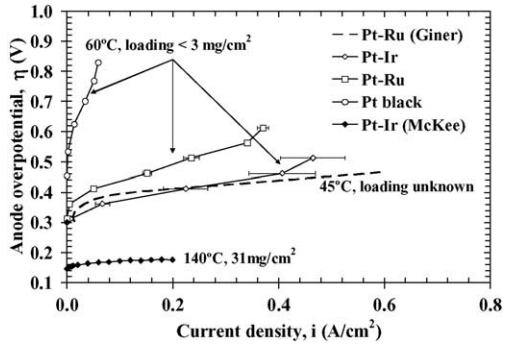

Fig. 5. Anodic polarization curves. Experiments at 60 °C in 1 M NH_3, 5 M KOH. Applied potential vs. Hg/HgO reference electrode. The use of electrodeposited bimetallic catalysts improves the kinetics of ammonia oxidation with Pt–Ir as the most active catalyst.

$$NH_{2,ads} + OH^- \Leftrightarrow NH_{ads} + H_2O + e^- \quad (4.2)$$

$$NH_{ads} + OH^- \Leftrightarrow N_{ads} + H_2O + e^- \quad (4.3)$$

$$NH_{x,ads} + NH_{y,ads} + (x+y)OH^- \Leftrightarrow N_2 + (x+y)H_2O + (x+y)e^- \quad (4.4)$$

$$2N_{ads} \Leftrightarrow N_2 \quad (4.5)$$

At low current densities, the oxidation of surface amine is considered to be rate-limiting (Eq. (4.2)), whereas at higher current densities (respectively high overpotentials) the recombination of adsorbed nitrogen is the limiting step (Eq. (4.5)) [8]. N_{ads} accumulates at the surface of the catalysts, blocking the active sites of noble metals and therefore acting as a poison toward the reaction. The observed trend in preferential adsorption of N_{ads} is given by Ru > Rh > Pd > Ir > Pt ≫ Au, Ag, Cu [9]. Dehydrogenation of ammonia occurs at a fast rate and at relatively low potentials on Ru (compared to Pt), which leads to a very fast deactivation of this catalyst.

However, on Pt–Ru, the presence of Pt allows the recombination of adsorbed nitrogen at a significant rate, either with itself (Eq. (4.5)) or with a partially dehydrogenated intermediate adsorbed on a Pt site (Eq. (4.4)). Low ratios of Ru in the deposit are needed to prevent the fast and complete dehydrogenation of ammonia to prevail over the recombination step on Pt. The bimetallic catalyst shows the combined benefit of a better activity (fast dehydrogenation rates on Ru at low potentials) and minimized deactivation (due to the presence of Pt). Ir is similar to Ru in the sense that dehydrogenation of ammonia occurs at lower potentials and faster than on Pt [9]. However, its stability toward deactivation is better (lower affinity to N_{ads}), which results in sustainable higher current densities at lower potentials when combined with Pt. It is likely that a higher concentration of Ir should increase the activity of the electrodeposit, and thus optimization of the deposit composition is scheduled for later studies. Clearly, Pt–Ir appears to be a suitable catalyst for the formation and recombination of partially dehydrogenated intermediates toward a sustainable production of nitrogen.

It is worth mentioning that the overpotential developed in the cathode was also measured (not shown in Fig. 5) and the maximum value reached was 0.15 V; consequently, the efficiency of the electrolysis process was limited by the anode over the entire range of current densities covered.

Also in Fig. 5, a comparison of current results on electrodeposited low-loading catalysts with former publications [13,14] on impregnated and thermally deposited Pt–Ru and Pt–Ir catalysts is presented. Although it was not the purpose here to develop optimized catalysts, it is seen that electrodeposited low-loading catalysts operating at low temperatures performed quite well in comparison. Further studies will focus on obtaining lower overpotentials as observed by McKee et al. [14] (at 140 °C and with a loading of 34 mg cm^{-2} on Pt–Ir catalysts) but with significantly lower loadings and at lower temperatures.

The results presented prove that it is possible to significantly reduce the amount of energy requested for the production of hydrogen from ammonia electrolysis by an appropriate selection of bimetallic catalysts and the optimization of their composition. It is now intended to present the efficiency of electrolytic cells built with such catalysts.

3.3.2. Polarization curve for the electrolytic cell and cell efficiency

The energy efficiency could be improved by choosing better performing electrocatalysts. From an economical point of view, it is necessary to evaluate the efficiency of the electrolytic cell. The polarization curve of the whole cell is shown in Fig. 6. These results were obtained at 60 °C in a stirred solution of 1 M NH_3, 5 M KOH with the electrode Pt–Ru as the counterelectrode for hydrogen evolution in an alkaline medium. The results not adjusted for IR drop show that voltages higher than 0.4 V are currently needed for hydrogen production.

According to the fact that the conversion of ammonia to hydrogen is 100% efficient (see Section 3.2), the energy ef-

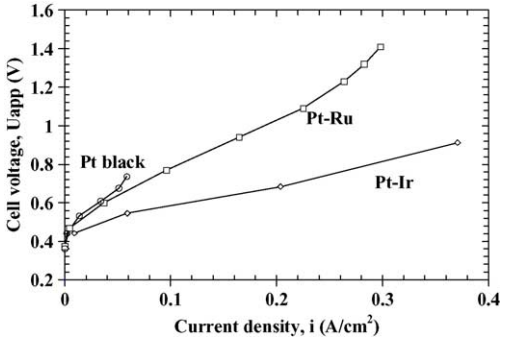

Fig. 6. Polarization curves for the ammonia electrolytic cell. Experiments at 60 °C in 1 M NH_3 and 5 M KOH. Cell voltages as low as 0.3 V are observed when Pt–Ir is used as an anode.

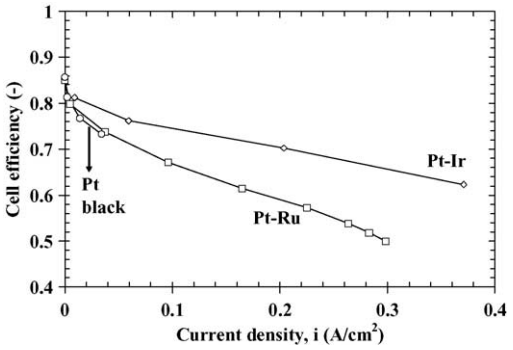

Fig. 7. Efficiency curves for ammonia electrolysis. Experiments at 60 °C, 1 M NH_3 and 5 M KOH. Efficiencies of 80% and higher can be obtained with the currently developed catalysts.

ficiency of the electrolytic cell can be expressed as

$$\varepsilon = \frac{3 \times \Delta H_{H_2}}{2 \times \Delta H_{NH_3} + 6 \times F\Delta E} \quad (5)$$

where ΔH_{H_2} is the lower heating value of hydrogen (242.7 kJ mol^{-1}), ΔH_{NH_3} the lower heating value of ammonia (320.1 kJ mol^{-1}), and ΔE the cell voltage. Defined in such a manner, the efficiency represents the amount of energy that could be obtained by burning the produced gas (lower heating value of hydrogen) divided by the amount of energy required to produce this gas (lower heating value of ammonia plus electrical energy needed to electrolyze ammonia). Such efficiency indicates the feasibility of the technology by comparing the energy that can be obtained from H_2 to the energy needed to produce it. The value of ε as a function of the hydrogen production rate (i.e. anodic current density) is given for selected catalysts in Fig. 7. The efficiency of ammonia transformation into hydrogen on Pt–Ir ranges from 80% at 10 mA cm^{-2} to 60% at 400 mA cm^{-2}. The theoretical efficiency (obtained for $\Delta E = 0.06$ V, which is thermodynamic cell voltage) is 108%. For comparison, the energy efficiency of an ammonia reformer runs between 60 and 70% [21] (this number does not include the energy required to compress the gas), showing the potential of the ammonia electrolysis technology to produce hydrogen in an energy-efficient manner. The high efficiency of the cell favors its integration with renewable energy (electricity) sources (e.g., wind and solar energy).

Fig. 8 compares the consumption of energy and power for the ammonia electrolytic cell to the ones for a commercial water electrolyzer [22] at different hydrogen production rates. The ammonia electrolytic cell operated at 25 °C with 1 M NH_3 and 5 M KOH, and Pt–Ir was used as anode. It can be observed that both the total energy consumption by the water electrolyzer as well as the power required are much higher than for the ammonia electrolytic cell (up to 65% higher). Fig. 8a also compares the energy consumed by the ammonia electrolytic cell with the energy produced by a commercial H_2 PEM fuel cell (from Arbin), as it can be seen the energy produced by the last is higher than the one required by the ammonia electrolytic cell up to a hydrogen rate of 0.033 g h^{-1}, that is, at lower hydrogen rates the H_2 PEM fuel cell could supply energy to the ammonia electrolytic cell with still some net energy (energy produced by H_2 PEM fuel cell minus energy consumed by the ammonia electrolytic cell) available. The energy consumed by the ammonia electrolytic cell can be brought even lower (according to the thermodynamics, see Fig. 8a) by improving the performance of the electrocatalyst. Research is being performed on this topic and it will be presented in future publications. Fig. 8b indicates that the maximum net power (power produced by H_2 PEM fuel cell minus power consumed by the ammonia electrolytic cell) is achieved between 0.010 and 0.020 g h^{-1} of hydrogen. The results shown in Fig. 8 indicate that the ammonia electrolytic cell has the potential to operate by stealing part of the energy of a PEM hydrogen fuel cell. Furthermore, the lower energy consumption when compared to a water electrolyzer indicates that the ammonia electrolytic cell can be operated by renewable energy sources to produce hydrogen on demand.

3.3.3. Study of the catalyst stability

As reported elsewhere [10], it was difficult to obtain stable current densities over time, particularly at low temperatures and high current densities. This is due to the slow deactivation of the electrode. It has already been mentioned that poisoning occurs at the surface of the catalysts, probably in the form of the adsorbed intermediate N_{ads}. Fig. 9 shows the plot of current density versus time as the potential was increased stepwise by 0.1 V starting from the rest potential. The limiting current density was never reached; rather, the current density decreased sharply when higher values were reached, showing that poisoning of the electrode occurred faster at higher overpotentials.

In an attempt to slow down the deactivation of the surface, the potential was varied in a stepwise manner as shown in Fig. 10. By applying a periodic cathodic pulse (E_{min}), it was expected that fully dehydrogenated nitrogen resulting from Eq. (4.5) would be reduced back to an active partially dehydrogenated intermediate. This test procedure was repeated in time until steady state was reached or until complete poisoning of the surface occurred. The purpose of this study was also to optimize the value of the parameters dt_1 (cathodic step time), dt_2 (anodic step time), and E_{min} for a chosen E_{max} (anodic potential), in order to provide a maximum stable current output. The results presented here were obtained with Pt–Ir electrode as an anode. The potential E_{max} was set at −0.35 V versus Hg/HgO and the step time dt_1 was set to 120 s.

By decreasing E_{min} to potentials more negative than −0.6 V (cathodic step time $dt_2 = 1$ s), one observed that the poisoning of the catalyst slowed down significantly (see Fig. 11). In fact, at 25 °C and for a resting potential E_{min} below −0.8 V, the anodic current was higher after 4 h of cycling (labeled as last cycle in Fig. 11) than it is at the beginning of the experiment (labeled as first cycle in Fig. 11). In Fig. 12, the cathodic currents obtained during the step at E_{min}

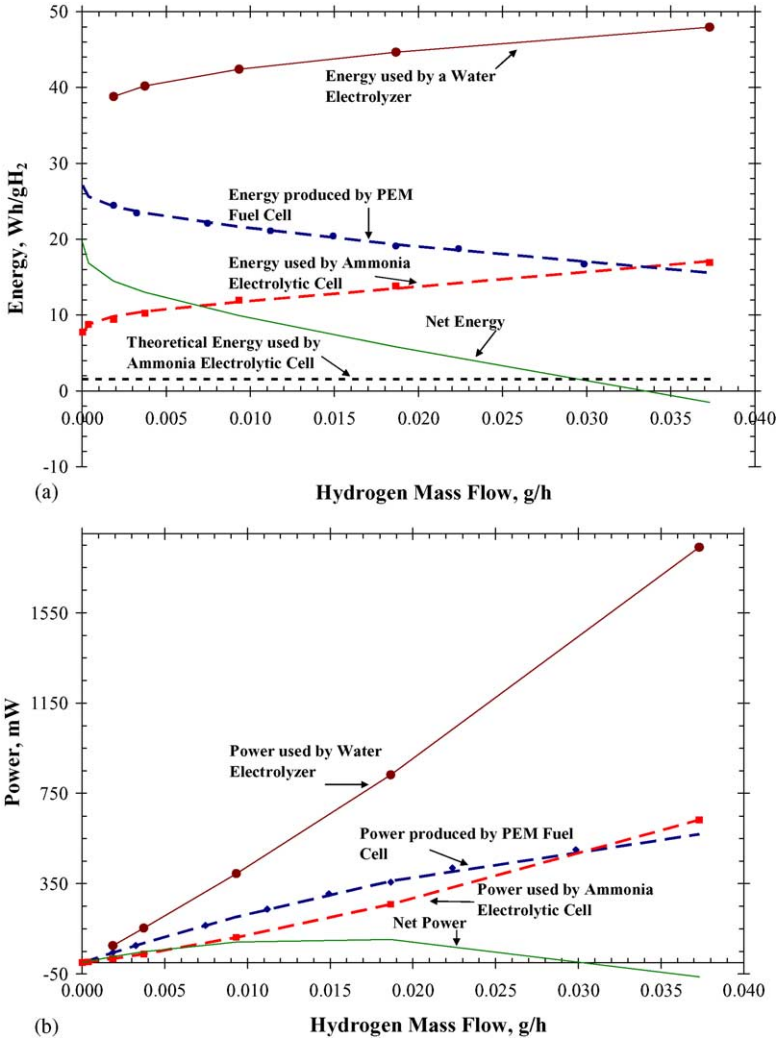

Fig. 8. Energy balance on an integrated system: ammonia electrolytic cell (prototype)/hydrogen PEM fuel cell (commercial) as a function of hydrogen rate. Ammonia electrolytic cell operated at 25 °C with 1 M NH_3 and 5 M KOH. Pt–Ir was used as anode. The ammonia electrolytic cell consumes less energy and power than the one produced by the H_2 PEM fuel cell and much lower energy and power than the one consumed by a commercial water electrolyzer: (a) energy of the system; (b) power of the system.

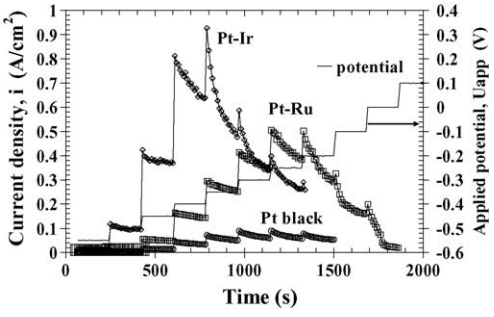

Fig. 9. Effect of poisoning on polarization curves. Experiments at 60 °C in 1 M NH_3, 5 M KOH. Applied potential vs. Hg/HgO reference electrode. Poisoning occurs faster at more positive potential, which can be explained by the preferential formation of adsorbed nitrogen on the surface of the catalysts.

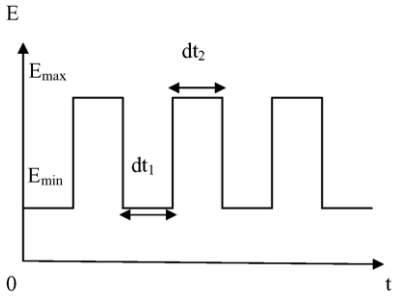

Fig. 10. Test procedure (potentiostatic steps) for remediation of catalyst poisoning during ammonia electrolysis.

of the last cycle (after 6 h of cycling) show that the reduction of at least one intermediate species occurred below −0.6 V versus Hg/HgO. The full reduction occurred as early as the first second following the cathodic step initiation (Fig. 13),

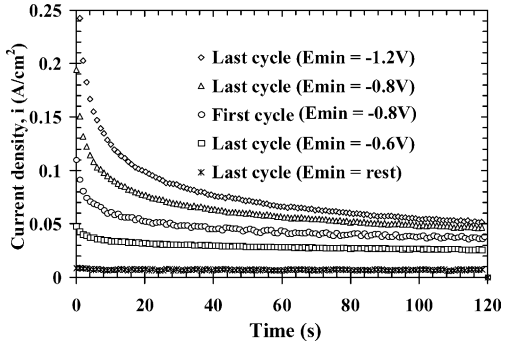

Fig. 11. Effect of E_{min} on the stability of the anodic current density. Pt–Ir was used as anode. Experiments at 25 °C in 1 M NH_3, 5 M KOH. Applied potential vs. Hg/HgO reference electrode. By periodically pulsing in the cathodic direction at potentials lower than the rest potential, the stability of the reaction of oxidation is observed over time.

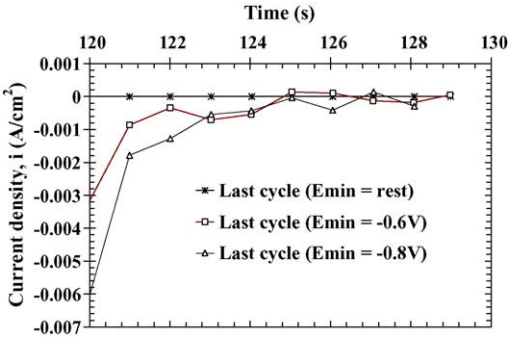

Fig. 12. Cathodic current densities during a potentiostatic step at E_{min}. Pt–Ir was used as anode experiments at 25 °C in 1 M NH_3, 5 M KOH. Applied potential vs. Hg/HgO reference electrode. The cathodic currents show that adsorbed species on the surface are reduced back to active intermediates.

which meant that the electrode was reactivated in such period of time. This technique proved that intermediates of reaction blocking the active surface could be reduced back to an active species toward sustainable nitrogen production.

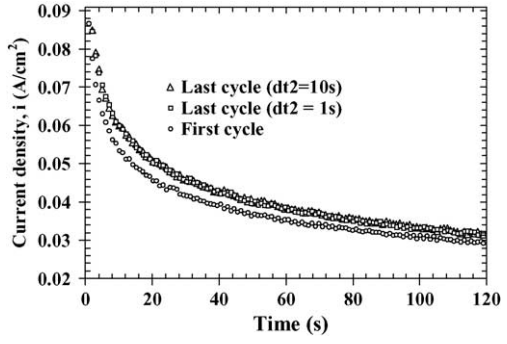

Fig. 13. Anodic current densities in time as a function of reduction time period dt_2. Pt–Ir was used as anode. Experiments at 25 °C in 1 M NH_3, 5 M KOH. The maximum reactivation of the surface is obtained after a cathodic pulse as short as 1 s.

4. Conclusions

The concept of an ammonia alkaline electrolytic cell for high-purity hydrogen production has been introduced. The technology offers high energy efficiency. The development of bimetallic catalysts by electrodeposition appears to be a promising technique for the production of low-loading active electrodes for low-temperature ammonia electrolysis. Bimetallic catalysts showed higher activity at lower overpotentials. An operating procedure for the electrolytic cell was developed, which prevents deactivation over a long period of time. Additional work on the optimization of catalyst preparation by electrodeposition (including the optimization of chemical composition) needs to be performed to improve the catalytic activity (lower the electrical energy consumption) and lower material cost. The results of the study indicate that the production of hydrogen by the electrolysis of ammonia is a promising technology as the thermodynamics is in favor of the reaction; however, the commercialization of the technology depends on the development of effective electrodes for the electro-oxidation of ammonia. Therefore, future work on this area should be focus on the development of electrodes to decrease the overpotential of this reaction.

Acknowledgements

The authors would like to acknowledge the financial support from the Office of the Vice President for Research, Ohio University, and the 1804 Fund Award by the Trustees of the Ohio University Foundation, the Department of Chemical Engineering, Ohio University, and the Stocker Research fellowship, Ohio University. The authors would also like to acknowledge the help of D. Ingram for the XPS and RBS studies funded by the W.M. Keck Foundation.

References

[1] R.A. Wynveen, Fuel Cells 2 (1963) 153–167.
[2] G. Strickland, Int. J. Hydrogen Energy 9 (1984) 759–766.
[3] S. Wasmus, E.J. Vasini, M. Krausa, H.T. Mishima, W. Vielstich, Electrochim. Acta 39 (1994) 23–31.
[4] G.G. Botte, F. Vitse, M. Cooper, Electro-catalyst for oxidation of ammonia in alkaline media and its application to hydrogen production, ammonia fuel cells, ammonia electrochemical sensors, and purification process for ammonia-contained effluents, Pending Patent (2003).
[5] E.L. Simons, E.J. Cairns, D.J. Surd, J. Electrochem. Soc. 115 (1969) 556–561.
[6] H.G. Oswin, M. Salomon, Can. J. Chem. 41 (1963) 1686–1694.
[7] T. Katan, R.J. Galiotto, J. Electrochem. Soc. 110 (1963) 1022–1023.
[8] H. Gerischer, A. Mauerer, J. Electroanal. Chem. 25 (1970) 421–443.
[9] A.C.A. de Vooys, M.T.M. Koper, R.A. van Santen, J.A.R. van Veen, J. Electroanal. Chem. 506 (2001) 127–137.
[10] K. Endo, K. Nakamura, T. Miura, Electrochim. Acta 49 (2004) 2503–2509.
[11] J. Ge, D.C. Johnson, J. Electrochem. Soc. 142 (1995) 3420–3423.

[12] M. Donten, W. Hyk, M. Ciszkowska, Z. Stojek, Electroanalysis 9 (1997) 751–754.
[13] J.D. Giner, J.R. Moser, Patent US 3,650,838 (1972) 1–4.
[14] D.W. McKee, A.J. Scarpellino Jr., I.F. Danzig, M.S. Pak, J. Electrochem. Soc. 116 (1969) 562–568.
[15] B.A. Lopez de Mishima, D. Lescano, T. Molina Holgado, H.T. Mishima, Electrochim. Acta 43 (1997) 395–404.
[16] F.J. Vidal-Iglesias, N. Garcia-Araez, V. Montiel, J.M. Feliu, A. Aldaz, Electrochem. Commun. 5 (2003) 22–26.
[17] D. Ives, G. Janz, Reference Electrodes: Theory and Practice, Academic Press, New York, 1961.
[18] M.S. Ureta-Zanartu, C. Yanez, M. Paez, G. Reynes, J. Electroanal. Chem. 405 (1996) 159–167.
[19] C.A. Marrese, Anal. Chem. 59 (1987) 217–218.
[20] T.J. Edwards, J. Newman, J. Prausnitz, AIChE J. 21 (1975) 248–259.
[21] R. Metkemeijer, Ph.D. dissertation, Ecole des Mines de Paris, 1994.
[22] S. Narayanan, W. Chun, B. Jeffries-Nakamura, T.I. Valdez, NASA Tech. Briefs 26 (2002) 19.